Letter

Antiferroelectricity in pure ferroelastics

Pierre Tolédano[1,*] and Gen Li[2]

[1]*Laboratory of Physics of Complex Systems, University of Picardie, 80000 Amiens, France*

[2]*Palace Museum, Beijing 100009, People's Republic of China*

(Received 9 December 2020; revised 1 June 2021; accepted 2 June 2021; published 14 June 2021)

In pure ferroelastics, the coupling existing under applied electric field between spontaneous strain and electric polarization is shown theoretically to transform the paraelastic and ferroelastic phases into polarized phases. This effect is rooted in the existence in the zero-field crystal structure of most ferroelastics of polarizable crystallographic sites forming an antiferroelectric array of dipoles. Under high fields the polar ferroelastic phase can become ferroelectric across a first-order isostructural transition, which exhibits a double hysteresis loop.

DOI: 10.1103/PhysRevB.103.L220101

Ferroelastic transitions are those reversible structural phase transitions that give rise to a spontaneous strain, preserving a group-subgroup relationship between the space-groups of the parent-paraelastic and daughter-ferroelastic phases [1–4]. They can occur in conjunction with ferroelectricity or as pure ferroelastic transitions, which form the largest class of structural ferroic transitions [3,4]. Two different situations are found in pure ferroelastics depending on whether the spontaneous strain has the symmetry of the primary transition order-parameter (proper ferroelastic) or constitutes a secondary order-parameter (improper ferroelastic) [5–7]. In the framework of the Landau theory, this latter situation is taken into account by the coupling $e\eta^f$ between the primary order-parameter η and the spontaneous strain e where the integer $f > 1$ is the faintness index of the spontaneous strain [8].

The elastic features of pure ferroelastic transitions are assumed to constitute their most specific properties [4,9], and their current theoretical description usually omits the coupling $e_{ij}P_iP_j$ between the strain tensor components e_{ij} and the product of electric polarization components P_iP_j. Using a Landau theoretical approach, we show that the activation of this coupling by an applied electric field substitutes the paraelastic and ferroelastic phases by polar phases. This effect is rooted in the set of polarizable crystallographic sites forming an antiferroelectric array of dipoles, which exists at zero fields in many ferroelastic and paraelastic structures. Under high fields, the polar ferroelastic phase can become ferroelectric across a first-order isostructural transition associated with a double hysteresis loop, conferring an antiferroelectric character to the ferroelastic transition.

Let us consider as an illustrative example the proper ferroelastic second-order transition taking place at 420 K in NdP_5O_{14} [10], with the orthorhombic-to-monoclinic space-group change $Pmna \rightarrow P2_1/b$, giving rise to a spontaneous shear strain e_{xy}. Taking into account the strain-polarization coupling $e_{xy}P_xP_y$ which implies a two-dimensional character for the corresponding electric-field-induced effects, the free energy associated with the transition under applied field **E** along the (x, y plane) reads

$$F_1 = \frac{\alpha}{2}e^2 + \frac{\beta}{4}e^4 + \frac{{P_x}^2}{2\chi_{0x}} + \frac{P_y^2}{2\chi_{0y}} + \delta e P_x P_y - E_x P_x - E_y P_y, \tag{1}$$

where $e = e_{xy}$ is the spontaneous strain, P_x, P_y are field-induced polarization components, δ is a coupling constant, $\alpha = a(T - T_c)$, and a, β, χ_{0x}, χ_{0y} are positive constants. The equations of state obtained by minimizing F_1 with respect to e, P_x, and P_y are

$$e(\alpha + \beta e^2) + \delta P_x P_y = 0, \tag{2}$$

$$\chi_{0x}^{-1}P_x + \delta e P_y = E_x, \tag{3}$$

$$\chi_{0y}^{-1}P_y + \delta e P_x = E_y. \tag{4}$$

At zero field the paraelastic ($e = 0, \alpha > 0$) and ferroelastic [$e_0 = \pm(-\alpha/\beta)^{1/2}, \alpha < 0$] phases are stable. Under applied field, the second-order transition between the zero-field phases is replaced by a first-order isostructural transition between polarized phases having the same monoclinic symmetry Pb and displaying the following polarization components:

$$P_x = \frac{\chi_{0x}E_x - \delta\chi_{0x}\chi_{0y}eE_y}{1 - \delta^2\chi_{0x}\chi_{0y}e^2}, \tag{5}$$

$$P_y = \frac{\chi_{0y}E_y - \delta\chi_{0x}\chi_{0y}eE_x}{1 - \delta^2\chi_{0x}\chi_{0y}e^2}, \tag{6}$$

where e is a real root of Eq. (2) depending on P_x and P_y. From Eqs. (5) and (6) one deduces the susceptibility tensor components $\chi_{ij} = \mathrm{Lim}_{E_j \rightarrow 0}\frac{P_i}{E_j}$:

$$\chi = \frac{1}{1 - \delta^2\chi_{0x}\chi_{0y}e_0^2}\begin{bmatrix} \chi_{0x} & -\delta\chi_{0x}\chi_{0y}e_0 \\ -\delta\chi_{0x}\chi_{0y}e_0 & \chi_{0y} \end{bmatrix}, \tag{7}$$

*pierre.toledano@wanadoo.fr

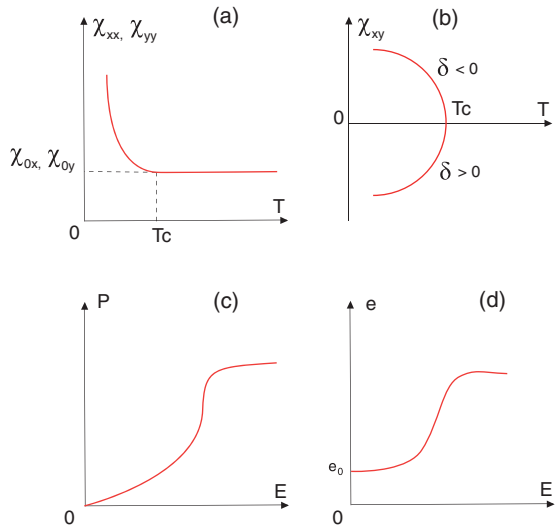

FIG. 1. Temperature dependence of the diagonal (a) and off-diagonal (b) components of the dielectric susceptibility χ from Eq. (7). In (b), $e_0 = +[\frac{a}{\beta}(T_c - T)]^{1/2}$. (c),(d) Electric field dependence of (c) the field-induced polarization $P(E)$ and (d) the ferroelastic shear strain $e(E)$ below T_c in the polarized ferroelastic phase. Assuming E along the diagonal of the (x, y) plane and $\chi_{0x} \approx \chi_{0y} = \chi_0$ yields $P = P_x = P_y \approx \frac{\chi_0 E}{1+\chi_0 \delta e}$, which, when inserted in Eq. (2), allows us to approximate $e(E)$, and subsequently $P(E)$. At low fields $e \approx e_0 - \delta\chi_0^2\alpha^{-1}E^2$, and at large fields $e \approx (-\frac{\delta\chi_0^2}{\beta+\delta^2\chi_0^2\alpha})^{1/3}E^{2/3}$.

where $e_0 = \pm[\frac{a}{\beta}(T_c - T)]^{1/2}$ is the spontaneous strain at zero field. Below T_c the diagonal components increase [Fig. 1(a)], whereas the off-diagonal components increase for $\delta < 0$ or decrease for $\delta > 0$ [Fig. 1(b)].

Therefore, an electric field substitutes the zero-field paraelastic-ferroelastic transition of NdP_5O_{14} by an isostructural transition between polar phases. This effect can be linked to the local changes occurring in NdP_5O_{14} at zero fields: In its ferroelastic phase, all crystallographic sites are at the Wyckoff positions (4*e*) with a triclinic polar site symmetry 1 [11], and these polar sites carry dipoles forming an antiferroelectric array consistent with the nonpolar overall symmetry $P2_1/b$ of the phase [Fig. 2(a)]. An electric field transforms the antiferroelectric structure into a polar configuration [Fig. 2(b)] with a macroscopic switchable polarization **P** [12,13]. The paraelastic phase of NdP_5O_{14} has also crystallographic sites with polar symmetries *m* (4*h*), 2 (4*e*, 4*f*), and 1 (8*i*) [11], forming an antiferroelectric arrangement which acquires a nonzero polarization under applied field.

Above and below T_c, the shear-strain e and polarization **P** of the field-induced phases have a different origin and dependence on the applied field. Above T_c, e is due to the lowering of symmetry of the paraelastic phase from orthorhombic *Pmna* to monoclinic Pb, and **P** corresponds to an orientational polarization of existing dipoles. Below T_c, e is a spontaneous ferroelastic strain and **P** results from the emergence of new dipoles. Figures 1(c) and 1(d) show the dependence of e and **P** in the ferroelastic phase below T_c.

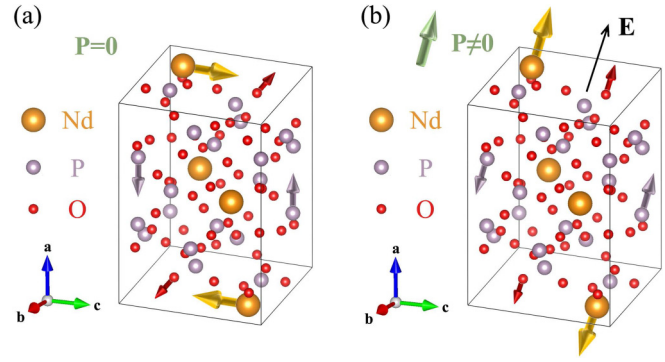

FIG. 2. Dipole configurations in the ferroelastic unit-cell of NdP_5O_{14} with atoms in Wyckoff positions (4e) and site symmetry 1. (a) Antiferroelectric zero-field configuration compatible with the macroscopic symmetry $P2_1/b$. (b) Field-induced configuration of symmetry Pb with E parallel to the (a, b) plane. A single dipole pair is represented for each type of atom.

Similar results are obtained for improper ferroelastic transitions. Consider, for example, the second-order transition occurring at 185 K in Hg_2Cl_2 [14] with the tetragonal-to-orthorhombic space-group change $I4/mmm \rightarrow Cmcm$ and the strain-polarization coupling $e_{xy}P_xP_y$. It is associated with a two-component order-parameter fulfilling the equilibrium conditions $(\eta_1 = \eta, \eta_2 = 0)$ [3], which yield the effective transition free-energy under applied field:

$$F_2 = \frac{\alpha}{2}\eta^2 + \frac{\beta}{4}\eta^4 - \mu\eta^2 e + c\frac{e^2}{2} + \delta e P_x P_y + \frac{P_x^2}{2\chi_{0x}} + \frac{P_y^2}{2\chi_{0y}} - E_x P_x - E_y P_y, \quad (8)$$

with $\mu > 0$, $c > 0$, and $\delta < 0$. The equations of state

$$\eta(\alpha + \beta\eta^2 - 2\mu e) = 0, \quad (9)$$

$$ce - \mu\eta^2 + \delta P_x P_y = 0, \quad (10)$$

and Eqs. (3) and (4) yield the equilibrium values at zero field for the paraelastic $(\eta = 0, e = 0, \alpha > 0)$ and ferroelastic phase $[\eta = \pm(\frac{-\alpha c}{\beta c - 2\mu^2})^{1/2}$, $e = \frac{\mu\eta^2}{c}$, $\alpha < 0$, $\beta c > 2\mu^2]$. Under applied field, both phases become monoclinic *Cm*, with the polarization components (P_x, P_y) given by Eqs. (5) and (6). The paraelastic phase exhibits a field-induced strain $e = -\frac{\delta}{c}P_xP_y$ due to the symmetry lowering *I*4/*mmm*-to-*Cm*. In the ferroelastic phase, η, e and P_x, P_y are mutually correlated with $\eta = \pm(\frac{-\alpha c - 2\mu\delta P_x P_y}{\beta c - 2\mu^2})^{1/2}$ and $e = \frac{\mu\eta^2 - \delta P_x P_y}{c}$.

Thus, under applied field the paraelastic and ferroelastic zero-field phases of Hg_2Cl_2 become polarized phases having different values of the strain and polarization. As for NdP_5O_{14}, the polar character of the phases in Hg_2Cl_2 is related to an orientational polarization of dipoles located at the Wyckoff positions (4*e*) in the paraelastic phase and (8*g*) in the ferroelastic phase, having, respectively, the polar site symmetries 4*mm* and *m* [15,16]. They form an antiferroelectric array of dipoles at zero fields [Fig. 3(a)], and a polarized structure with a macroscopic polarization oriented along the field [Fig. 3(b)].

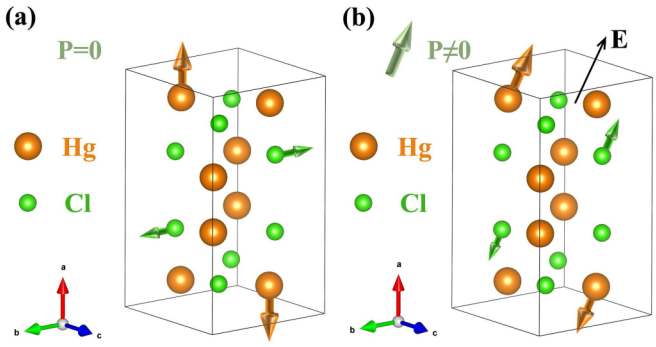

FIG. 3. Dipole configurations in the ferroelastic unit-cell of Hg_2Cl_2 with atoms in Wyckoff positions (8*g*) and site symmetry *m*. (a) Antiferroelectric zero-field configuration compatible with the macroscopic *Cmcm* symmetry. (b) Field-induced configuration of symmetry *Cm*, with *E* parallel to the (*a,b*) plane. A single dipole pair is represented for each type of atom.

The properties found for the two considered examples of ferroelastic transitions shed light on the role played by the local dipolar order existing at zero fields in this ferroic class of compounds. Column (e) of Table I indicates for the ferroelastic materials listed in column (a) the crystallographic site symmetries in the ferroelastic and paraelastic phases of about 30 pure ferroelastic transitions. It shows that except for AuCu and InTl, all transitions exhibit emerging polar crystallographic sites in the ferroelastic phase. Moreover, with the exception of $SrTiO_3$, $LaAlO_3$, $CdSnAs_2$, AuCu, and InTl, the paraelastic phases possess polar site symmetries as well. The emergence of polar sites at the local scale is connected to the macroscopic symmetry-breaking mechanism. It suggests that for a large number of pure ferroelastic transitions, the spontaneous deformation of the crystal may originate in the dipolar order emerging below T_c.

The conceptual image of electric dipoles localized at polar crystallographic sites must be specified for the zero-field ferroelastic structures. For proper ferroelastic transitions where the number of atoms in the elementary crystal unit-cell is preserved, one can separate in each ferroelastic unit-cell two regions corresponding to antiparallel local polarizations. The dipoles are localized at sites consistent with the symmetry operations of the ferroelastic structure and representing the polarization of the entire regions. For improper ferroelastic transitions, which display a breaking of the translational periodicity, the zero-field antiferroelectric structure can be considered as formed by an alternation of unit-cells having antiparallel local polarizations.

Thus, for a majority of pure ferroelastics, the activation of the strain-polarization couplings under applied field, given in column (d) of Table I, results from the antiferroelectric order existing at zero field. This property provides a clue for understanding why notable antiferroelectric materials, such as $PbZrO_3$, $NaNbO_3$, $NH_4H_2PO_4$, or C_4O_4H, belong to this class of ferroics [17,18]. Indeed, for most of the materials listed in column (a) the symmetry properties of the local crystallographic sites reported in columns (e) and (f) of Table I verify the conditions proposed in Ref. [19] for a structural transition between nonpolar phases to qualify as antiferroelectric. These conditions assume that a set of crystallographic sites

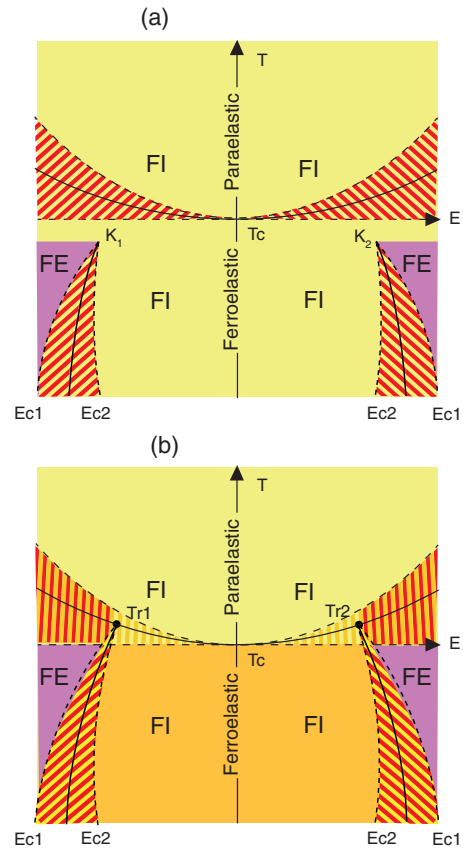

FIG. 4. Theoretical temperature–electric-field (TE) phase diagrams associated with the free energies given by (a) Eq. (1) and (b) Eq. (8). They contain regions of stability of the polarized (FI) and ferroelectric (FE) phases and hatched regions of coexistence between two phases. Solid and hatched curves are the first-order transition and the limit of stability curves, respectively. The E_{c1} and E_{c2} curves correspond to the coercive fields of the ferroelectric double hysteresis loop. In part (a), K_1 and K_2 are critical end points of the liquid-vapor type located at $T_K = T_c - \frac{27}{4a}\delta^2\beta P_x^2 P_y^2$. In part (b), Tr1 and Tr2 are triple points joining at high fields the isostructural ferroelectric transition curve and the isostructural paraelastic-ferroelastic transition curve.

undergoes a symmetry lowering resulting in the emergence of new polar sites, and that the space group of the ferroelastic phase has a symmorphic polar subgroup coinciding with the symmetry of the emerging polar sites.

However, only a small number of real ferroelastic materials fulfilling the preceding conditions exhibit the most distinctive dielectric property typifying antiferroelectrics, which consists of a double hysteresis loop associated with a first-order transition to a high-field ferroelectric phase from the low-field polar phase [19,20]. In our theoretical description, a transition from a polarized ferrielectric-like phase, with dipoles paired in the opposite sense, to a ferroelectric phase, with all dipoles in the same sense, has an isostructural character, as both phases display the same macroscopic symmetry. In NdP_5O_{14} the two phases have the space group Pb, with distinct equilibrium values of *e* verifying Eq. (2). In Hg_2Cl_2 two distinct values of η deduced from Eqs. (9) and (10) are associated with isostructural phases of symmetry *Cm*. But other prerequisites have

TABLE I. For each ferroelastic material listed in column (a), the columns give (b) the transition temperature at zero field in degrees Kelvin; (c) the space-group change at the transition; (d) the coupling between the spontaneous strain and polarization components; (e) the point-group symmetry of the polar crystallographic sites emerging in the ferroelastic phase at zero field, and the symmetry of the corresponding sites in the paraelastic phase; (f) the symmorphic polar subgroups of the ferroelastic phase having the same point-group as the polar sites emerging in the ferroelastic phase; and (g) a reference.

A. Proper ferroelastic transitions

(a)	(b)	(c)	(d)	(e)	(f)	(g)
NdP_5O_{14}	420	$Pmna \rightarrow P2_1/b$	$e_{xy}P_xP_y$	(4h) m → 1 (4e), (4f) 2 → 1 (4e)	P1	[12]
$BiVO_4$	528	$I4_1/a \rightarrow B2/b$	$(e_{xx}-e_{yy})(P_x^2-P_y^2)$, $e_{xy}P_xP_y$	(4a,4b) 4_ → 2 (4e)	C2	[21]
TeO_2	8kbar	$P4_12_12 \rightarrow P2_12_12_1$	$(e_{xx}-e_{yy})(P_x^2-P_y^2)$	(4a) 2 → 1 (4a)	P1	[22]
$TbVO_4$	33	$I4_1/amd \rightarrow Fddd$	$e_{xy}P_xP_y$	(16h) m → 1 (32h)	P1	[23]
$DyVO_4$	14	$I4_1/amd \rightarrow Imma$	$(e_{xx}-e_{yy})(P_x^2-P_y^2)$	(4a, 4b) 4_m 2 → mm2 (4e)	Imm2	[24]
NaN_3	293	R3_m → B2/m	$(e_{xx}-e_{yy})(P_x^2-P_y^2)$	(6c) 3m → m (4i)	Cm	[25]
KNO_2	295	Fm3_m → R3_m	$e_{yz}P_yP_z+e_{zx}P_zP_x+e_{xy}P_xP_y$	(4a) m3_m → m (18h)	Cm	[26]
$RbAg_4I_5$	208	$P4_132 \rightarrow R32$	idem	(4a) 32 → 2 (3e)	C2	[27]
$K_2Mn_2(SO_4)_3$	200	$P2_13 \rightarrow P2_12_12_1$	$(e_{xx}-e_{yy})(P_x^2-P_y^2)+(2e_{zz}-e_{xx}-e_{yy})(2P_z^2-P_x^2-P_y^2)$	(4a) 3 → 1 (4a)	P1	[28]
KCN	170	Fm3_m → Immm	idem	(24e) 4mm → m2m (4h)	Imm2	[29]
InTl	320	Fm3_m → I4/mmm	idem	(4a) m3_m → 4/mmm (2a)	None	[30]
$NiCr_2O_4$	274	Fm3_m → $I4_1/amd$	idem	(32e) 3m → m (16h)	Cm	[31]

B. Improper ferroelastic transitions

(a)	(b)	(c)	(d)	(e)	(f)	(g)
$C_4O_4H_2$	470	I4/m → $P2_1/m$	$e_{xy}P_xP_y$, $(e_{xx}-e_{yy})(P_x^2-P_y^2)$	(2a, 2b) 4/m → m (2e) (4c) 2/m → m (2e)	Pm	[32]
ADP	148	$I4\_2d \rightarrow C222_1$	$(e_{xx}-e_{yy})(P_x^2-P_y^2)$	(4a, 4b) 4_ → 1 (4a)	P1	[33]
$RbFeF_4$	570	P4/mmm → Pmma	idem	(1a) 4/mmm → m (4d) (2e) mmm → 2 (4c)	Pm P2	[34]
VO_2	343	$P4_2/mnm \rightarrow P2_1/b$	$e_{yz}P_yP_z$, $(e_{xx}-e_{yy})(P_x^2-P_y^2)$	(2a) mmm → 1 (4e) (4f) m2m → 1 (4e)	P1	[35]
Hg_2Cl_2	185	I4/mmm → Cmcm	$e_{xy}P_xP_y$	(4e) 4mm → m (8g)	Cm	[14]
$Pb_3(PO_4)_2$	453	R3_m → B2/b	idem	(3a) 3_m → 2 (4e) (6c) 3m → 1 (8f) (18h) m → 1 (8f)	C2 P1	[36]
$CdSnAs_2$	840	F4_3m → I4_2d	$(2e_{zz}-e_{xx}-e_{yy})(2P_z^2-P_x^2-P_y^2)$	(4a) 4_3m → 2 (8d)	C2	[37]
$SrTiO_3$	196	Pm3_m → I4/mcm	idem	(3c) 4/mmm → m 2m (8h)	Fmm2	[38]
NH_4Br	235	Pm3_m → P4/nmm	idem	(1b) m3_m → 4 mm (2c)	P4mm	[39]
CuAu	653	Fm3_m → P4/mmm	idem		No	[40]
$LaAlO_3$	808	Pm3_m → R3_c	$e_{yz}P_yP_z$,$e_{xz}P_xP_z$, $e_{xy}P_xP_y$	(3d) 4/mmm → 2 (18e)	C2	[41]
$PbZrO_3$	505	Pm3_ m → Pbam	$(e_{xx}-e_{yy})(P_x^2-P_y^2)$ $+(2e_{zz}-e_{xx}-e_{yy})(2P_z^2-P_x^2-P_y^2)$	(1b) m3_m → m (4g,4h) (1a)m3_m → 1 (8i) (3d)4/mmm → m (4g,4h) (3d)4/mmm → 2(4f,4e),1(8i)]	Pm P1 Pm P2, P1	[18]
$NaNbO_3$	913	Pm3_m → P4/mbm	$(2e_{zz}-e_{xx}-e_{yy})(2P_z^2-P_x^2-P_y^2)$	(1a,1b): m3_m → m 2m (4g)	Cmm2	[18]
	848	→ Cmcm	idem $+e_{xy}P_xP_y$	→ m 2m(4c) → 2(8e),m(8f,8g)	Amm2 C2,Pm,Cm	
	793	→ Pmmn	$(e_{xx}-e_{yy})(P_x^2-P_y^2)$ $+(2e_{zz}-e_{xx}-e_{yy})$	→ mm 2(2a) → m (4e)	Pmm2 Pm	
	733	→ Pmmn	idem	→ mm 2(2a,2b) → m (4e)	Pmm2 Pm	
	633	→ Pbcm	idem	→ m (4d), 2(4c)	Pm,P2	

to be taken into account in real ferroelastic materials for the stabilization of a ferroelectric phase. In particular, the energy barrier corresponding to the isostructural transition should be overcome.

Figures 4(a) and 4(b) show theoretical temperature–electric-field phase diagrams associated, respectively, with the free energies F_1 and F_2, assuming the stabilization of a high field ferroelectric transition below T_c. In both phase diagrams, the paraelastic-ferroelastic second-order transition at zero field becomes a first-order isostructural transition under applied fields. In the phase diagram of Fig. 4(a) the isostructural transition to the ferroelectric phase has a critical end point of the liquid-vapor type around which the dipoles reorient continuously from a ferrielectric-like configuration to the ferroelectric configuration and vice versa. In the phase diagram of Fig. 4(b), the ferroelectric transition curve joins the ferroelastic transition curve at triple points.

In summary, the existence of field-induced polarized phases appears as an intrinsic property of most pure ferroelastics. At the macroscopic level, this property derives from the specific strain-polarization coupling distinguishing this class of structural ferroics. At the microscopic level, the property is rooted in the local dipolar antiferroelectric configurations of the phases at zero fields. The realization of a ferroelectric transition at high fields and the related double hysteresis loop, which is a benchmark for antiferroelectricity, requires suitable symmetry and energy conditions.

A recently proposed theory of antiferroelectric phase transitions [19] considers the bi-quadratic coupling $\eta^2 P^2$ between the primary transition order-parameter and the field-induced polarization, which exists for all structural transitions between nonpolar phases. The influence of such coupling on pure ferroelastic transitions depends on its relative magnitude with respect to the specific ferroelastic strain-polarization coupling. Note that for improper ferroelastics with a faintness index $f = 2$, one has $e \approx \eta^2$ and the $\eta^2 P^2$ coupling is equivalent to eP^2. The results obtained in Ref. [19] differ from the results of the present work because of the symmetry of the high field ferroelectric phase, which is exclusively determined by the orientation of the applied electric field, whereas in the present work it also depends on the spontaneous strain which couples to the polarization. Nevertheless, both descriptions have in common the essential role played by the underlying antiferroelectric dipolar order existing in the absence of applied field. It suggests that in parallel to the traditional ferroic classification based on tensorial properties, one may classify structural ferroic phase transitions in terms of their ferroelectric or antiferroelectric dipolar order at zero fields, analogous to the ferromagnetic and antiferromagnetic classes of magnetic phase transitions.

The authors are grateful to Bruno Mettout, Steve Lange, Dmitry Khalyavin, and Jean-Claude Tolédano for helpful discussions.

[1] K. Aizu, J. Phys. Soc. Jpn. **27**, 387 (1969).
[2] J. C. Tolédano, Ann. Telecommun. **29**, 249 (1974).
[3] J. C. Tolédano and P. Tolédano, Phys. Rev. B **21**, 1139 (1980).
[4] E. K. H. Salje, *Phase Transitions in Ferroelastics and Co-elastic Crystals* (Cambridge University Press, Cambridge, 1993).
[5] V. Janovec, V. Dvorak, and J. Petzelt, Czech. J. Phys. B **25**, 1362 (1975).
[6] V. Dvorak, Suppl. J. de Physique **33**, C2 (1972).
[7] A. P. Levanyuk and D. G. Sannikov, Sov. Phys. Usp. **17**, 199 (1975).
[8] J. C. Tolédano and P. Tolédano, *The Landau Theory of Phase Transitions* (World Scientific, Singapore, 1987).
[9] P. Toledano, M. M. Fejer, and B. A. Auld, Phys. Rev. B **27**, 5717 (1983).
[10] J. P. Budin, A. Milatos-Roufos, N. Duc-Chinh, and G. L. Roux, J. Appl. Phys. **46**, 2867 (1975).
[11] A. J. Cramer and J. M. Cole, J. Solid State Chem. **266**, 250 (1989).
[12] C. F. Pulvari, Phys. Rev. **120**, 1670 (1960).
[13] Z. Fu, X. Chen, Z. Li, T. Hu, L. Zhang, P. Lu, S. Zhang, G. Wang, X. Dong, and F. Xu, Nat. Commun. **11**, 3809 (2020); K. Du, L. Guo, J. Peng, X. Chen, Z.-N. Zhou, Y. Zhang, T. Zheng, Y.-P. Liang, J.-P. Lu, Z.-H. Ni, S.-S. Wang, G. Van Tendeloo, Z. Zhang, S. Dong, and H. Tian, npj Quantum Mater. **5**, 49 (2020).
[14] C. Barta, A. A. Kaplyanskii, V. V. Kulakov, and Yu. F. Markov, Sov. Phys. Solid State **17**, 717 (1975).
[15] M. E. Bolko, M. D. Sharkov, A. M. Bolko, and S. G. Konnikov, Cryst. Rep. **63**, 196 (2018).
[16] N. J. Carlos, C. H. L. Kennard, and R. L. Davis, Z. Kristallogr. **187**, 305 (1989).
[17] K. M. Rabe, in *Functional Metal Oxides: New Science and Novel Applications*, edited by S. Ogale and V. Venkateshan (Wiley, New York, 2013).
[18] P. Tolédano and D. D. Khalyavin, Phys. Rev. B **99**, 024105 (2019).
[19] P. Tolédano and M. Guennou, Phys. Rev. B **94**, 014107 (2016).
[20] V. Känzig, *Ferroelectrics and Antiferroelectrics* (Academic, New York, 1957).
[21] J. D. Bierlein and A. W. Sleight, Solid State Commun. **16**, 69 (1975).
[22] P. S. Peercy and I. J. Fritz, Phys. Rev. Lett. **32**, 466 (1974).
[23] J. Pellicer-Porres, D. Vázquez-Socorro, S. López-Moreno, A. Muñoz, P. Rodríguez-Hernández, D. Martínez-García, S. N. Achary, A. J. E. Rettie, and C. B. Mullins, Phys. Rev. B **98**, 214109 (2018).
[24] K. Kishimoto, T. Ishikura, H. Nakamura, Y. Wakabayashi, and T. Kimura, Phys. Rev. B **82**, 012103 (2010).
[25] G. J. Simonis and C. E. Hathaway, Phys. Rev. B **10**, 4419 (1974).
[26] J. K. Solbakk and K. O. Stromme, Acta Chem. Scand. **23**, 300 (1969).
[27] F. L. Lederman, M. B. Salamon, and H. Peisl, Solid State Commun. **19**, 147 (1976).

[28] T. Hikita, J. Phys. Soc. Jpn. **43**, 1327 (1977).
[29] J. M. Rowe, J. J. Rush, and E. Prince, J. Chem. Phys. **66**, 5147 (1977).
[30] D. J. Gunton and J. A. Saunders, Solid State Commun. **12**, 569 (1973).
[31] O. Crottaz, F. Kubel, and H. Schmid, J. Mater. Chem. **7**, 143 (1997).
[32] E. J. Samuelsen and D. Semmingsen, Solid State Commun. **17**, 217 (1975).
[33] F. Jona and G. Shirane, *Ferroelectric Crystals* (Pergamon, New York, 1962).
[34] M. Hidaka, J. G. Wood, B. M. Wanklyn, and B. J. Gerrard, J. Phys. C **12**, 1799 (1979).
[35] J. R. Brews, Phys. Rev. B **1**, 2557 (1970).
[36] C. Joffrin, M. Lambert, and G. Pepy, Solid State Commun. **21**, 853 (1977).
[37] W. D. C. B. Gunatileke, D. Hobbis, H. Poddig, A. Tinkess, M. Beekman, H. Wang, K. Wei, R. E. Baumbach, and G. S. Nolas, Inorg. Chem. **59**, 3079 (2020).
[38] E. Pytte and J. Feder, Phys. Rev. **187**, 1077 (1969).
[39] W. Press, J. Eckert, D. E. Cox, C. Rotter, and W. Kamikatahara, Phys. Rev. B **14**, 1983 (1976).
[40] C. S. Barrett and T. B. Massalski, *The Structure of Metals* (McGraw Hill, New York, 1966).
[41] J. Axe, G. Shirane, and K. A. Muller, Phys. Rev. **183**, 820 (1969).